ANTIOXIDANTS & REDOX SIGNALING
Volume 10, Number 8, 2008

DOI: 10.1089/ars.2008.2042

Original Research Communication

Adeno-sh-β-Catenin Abolishes Ischemic Preconditioning–Mediated Cardioprotection by Downregulation of Its Target Genes VEGF, Bcl-2, and Survivin in Ischemic Rat Myocardium

MAHESH THIRUNAVUKKARASU,[1,2] ZHIHUA HAN,[3] LIJUN ZHAN,[1]
SURESH VARMA PENUMATHSA,[1] VENUGOPAL P. MENON,[2] and NILANJANA MAULIK[1]

ABSTRACT

β-Catenin, the downstream target of glycogen synthase kinase-3β (GSK-3β), plays a vital role in ischemic preconditioning (IP)-mediated cardioprotection. In the present study, we investigated the mechanism of IP-mediated cardioprotection through suppression of β-catenin expression by intramyocardial injection of adeno-sh-RNA against β-catenin (BCT) (4×10^8 pfu). Adeno-LacZ (LZ) was used as control. The rats were randomized into (a) LZ + ischemia–reperfusion (IR); (b) LZIPIR; (c) BCTIR; and (d) BCTIPIR. Isolated hearts from each group were subjected to 30 min of I followed by 2 h of R. Both IPIR group hearts were subjected to IP (5 min I + 10 min R; four cycles) before IR. Significant reduction in left ventricular functional recovery (78 *vs.* 88 mm Hg), dp/dt_{max} (1,802 *vs.* 2,189 mm Hg/sec), and aortic flow (4 *vs.* 9 ml/min) was observed in BCTIPIR compared with LZIPIR at 120 min of reperfusion. Increased infarct size (42 *vs.* 24%) and apoptotic cardiomyocytes (122 *vs.* 58 counts/60 HPF) were observed in BCTIPIR compared with LZIPIR. Real-time PCR and Western blot analysis showed significant downregulation in mRNA and protein expression of VEGF, Bcl-2, and survivin in BCTIPIR compared with LZIPIR. These findings indicated for the first time that silencing β-catenin abolished IP-mediated cardioprotection, probably through inhibition of VEGF-Bcl-2 and survivin. *Antioxid. Redox Signal.* 10, 1475–1485.

INTRODUCTION

Ischemic preconditioning (IP) (brief intermittent periods of ischemia and reperfusion) is a powerful endogenous phenomenon that generates profound protection against a sublethal prolonged episode of ischemia–reperfusion (26). IP is found to be cardioprotective in all the species studied, including humans (2, 40). Several signal-transduction pathways have been implicated in IP, which includes (but is not limited to) protein kinase C, nitric oxide, cGMP-dependent protein kinase, *Akt* (protein kinase B), ERK and p38 MAP kinases, AMP-dependent protein kinase, and the mitochondrial ATP-sensitive potassium channel (9, 15, 18). Recently it was reported that IP can mediate angiogenic and antiapoptotic effects *via* growth factors and receptors stimulation during MI, which is potentially a very exciting strategy for cardioprotection (11, 22).

A recent study from our laboratory documented for the first time that IP improves regional myocardial function, sig-

[1]Molecular Cardiology and Angiogenesis Laboratory, Department of Surgery, University of Connecticut Medical Center, Farmington, Connecticut.
[2]Department of Biochemistry and Biotechnology, Annamalai University, India.
[3]Department of Biochemistry and Molecular Biology, East Tennessee State University, Johnson City, Tennessee.

nificantly, along with increased capillary and arteriolar density after induction of survival factors such as vascular endothelial growth factor (VEGF), Bcl-2, and survivin in established chronic rat myocardial infarction model (11). Of several signaling pathways involved in IP-mediated cardioprotection, phosphatidylinositol 3 kinase (PI3-kinase) and its downstream targets play a very important role (37). Ischemic preconditioning–mediated downstream targets of PI3-kinase include the phosphorylation of the PKB/Akt pathway and the phosphorylation of glycogen synthase kinase-3β (GSK-3β) (21). This GSK-3β belongs to a family of conserved serine/threonine kinases present in eukaryotes, and its activity is regulated by various pathways other than the PI3-kinase-PKB/Akt-dependent pathway (39), such as Wnt signaling. Phosphorylation of GSK-3β results in the release, stabilization, and subsequent accumulation of β-catenin in the cytosol, followed by its translocation into the nucleus (7). β-Catenin is found to be a critical mediator during development and angiogenesis (24), and it is phosphorylated by active GSK-3β (nonphosphorylated) in a cytosolic multiprotein degradation complex containing adenomatous polyposis coli protein (APC), axin, and GSK-3β (1, 17, 24, 32). The phosphorylation of β-catenin thus marks it for ubiquitination and subsequent degradation by the proteosomal pathway. Therefore, when phosphorylation of β-catenin is blocked, it stabilizes, accumulates, and translocates into the nucleus, where it forms a complex with T-cell transcription factors/lymphoid-enhancer binding factor (TCF/LEF) and is able to activate or repress several important target genes, such as c-Myc, cyclin D1, fibronectin, VEGF, Bcl-2, and survivin (3, 4, 8, 27). Tong *et al*. (38) showed recently that IP resulted in phosphorylation and inactivation of GSK-3β, whereas pharmacologic preconditioning with lithium or SB216763, inhibitor of GSK-3β, mimicked IP-mediated cardioprotection in isolated rat hearts. Unlike most protein kinases, GSK-3β is constitutively active, and phosphorylation of GSK-3β leads to inhibition of its activity (21). Therefore, the activation of the PI3-kinase pathway leads to phosphorylation and thus inhibition of GSK-3β activity, resulting in accumulation of cytoplasmic β-catenin, which becomes available to bind to the TCF/LEF family of transcription factors and to induce target-gene expression. Thus, the key factors in β-catenin signaling are its stabilization and accumulation in the cytoplasm.

β-Catenin regulation in endothelial cells is found to be dependent on GSK-3β activity but independent of PI-3kinase/Akt activation, consistent with observations in other cell types (33). Importantly, wild-type β-catenin is found to promote angiogenesis, and the nonphosphorylated mutant of β-catenin is more effective than wild-type in promoting capillary formation (33). Moreover, the antiangiogenic phenotype conferred by transduction with constitutively active GSK3β was partly reversed by co-transduction with β-catenin (33).

Given the critical role of β-catenin, present study documented for the first time that a regulation of a novel β-catenin signaling pathway during IP is sufficient to promote cardioprotection. This was again validated by *in vivo* gene silencing mediated by the specific shRNA targeted against β-catenin and its effect on cell survivability, infarct size, and cardiac function followed by cardioprotection.

MATERIALS AND METHODS

Animal maintenance

Animals used in this study received humane care in compliance with the principles of the laboratory animal care formulated by the National Society for Medical Research and Guide for the Care and Use of Laboratory Animals prepared by the National Academy of Sciences and published by the National Institutes of Health (publication number NIH 85-23, revised 1985). Male Sprague–Dawley rats weighing between 275 and 300 g were used for the study.

Construction of adeno-shRNA-β-catenin (Ad-sh-β-cat)

We generated the sh-β-cat through a DNA vector–based strategy that synthesizes short-hairpin RNA (shRNA) from the U6 promoter, which has been found to be much more stable than siRNA in an *in vivo* system (35). The target sequences (gttgtcaatttgattaactat) corresponding to β-catenin mRNA (GenBank Accession No: AF121265) were designed empirically, and they started with G and contained no homology with other genes, as analyzed by Blast search. First the pBS/U6-sh-βcat vector was generated by a triple ligation of the following three DNA fragments:

1. The PCR fragment amplified from primers gccagggttttccagtcacgacg (P1) and cagcaagcttgaattagttaatcaaattgacaacaaacaaggcttttctccaagggata (P2) and template pBS/U6, and digested with *Kpn*I and *Hin*dIII;
2. The fragment annealed from agcttatagttaatcaaattgacaacttttg and aattcaaaaagttgtcaatttgattaactata;
3. pBluescript (SK) digested with *Eco*RI and *Kpn*I.

In effect, this method (34) recreated the pSilencer 1.0-U6 system (Ambion, Austin, TX) but has the added advantages of creating an shRNA that has clean ends unencumbered by any restriction site and has a mismatch that favors the antisense strand loading onto RISC over the sense strand. The pBS/U6-sh-βcat was subsequently used to generate a recombinant adenovirus, by using AdEasy system (Qbiogene, CA). Specifically, the U6-sh-βcat sequence was subcloned into pShuttle MCS *via* *Kpn*I and *Eco*RV. From the shuttle vector, the U6-sh-βcat was transferred into pAdEasy-1 by homology recombination in bacteria to generate a recombinant virus that expresses sh-βcat.

Experimental design

The rats were randomized into four groups: (a) Adeno-LacZ (LZ) + ischemia–reperfusion (LZIR); (b) LZ + ischemic preconditioning (IP) + ischemia–reperfusion (LZIPIR); (c) Ad-sh-β-catenin (BCT) + ischemia–reperfusion (BCTIR); and (d) Ad-sh-β-catenin (BCT) + ischemic preconditioning + ischemia–reperfusion, (BCTIPIR). Rats were anesthetized with ketamine HCl (100 mg/kg, i.p) and xylazine (10 mg/kg, i.p). Cefazolin (25 mg/kg, i.p) was administered by as preoperative antibiotic cover. Rats were intubated and placed in a supine position, and the body temperature was maintained at 37°C by means of a water-circulating thermal heating pad. An intercostal

thoracotomy in the left fourth intercostal space was performed under aseptic conditions. The heart was exposed, and the pericardium incised. A single dose of 100 μl shRNA against β-catenin (4×10^8 pfu) or Ad-LacZ (4×10^8 pfu) was injected at four different spots into the anterior wall of the left ventricle. Slight bulging and blanching of the epicardial surface verified the deposition of the suspension. After injection, the chest wall was closed in layers, as described previously by Kaga *et al.* (21). After surgery, analgesic buprenorphine (0.1 mg/kg, s.c.) was given, and the rats were weaned from the respirator; the rats were placed on a heating pad while recovering from anesthesia. Seventy-two hours after surgery, the rats were reanesthetized with sodium pentobarbital, and the hearts were excised to prepare isolated working hearts, as described in the subsequent section

Isolated working heart preparation

Rats were first anesthetized with sodium pentobarbital [80–100 mg/kg body weight (bw), i.p. injection (Abbott Laboratories, Abbot Park, IL) and heparinized (500 U/kg bw, i.p. injection; Elkins-Sinn, Inc., Cherry Hill, NJ). The heart was excised and immediately immersed in ice-cold perfusion buffer. The perfusion buffer consisted of a modified Krebs–Henseleit bicarbonate buffer [KHB buffer; composed of (in m*M*) 118 NaCl, 4.7 KCl, 1.2 $MgSO_4$, 25 $NaHCO_3$, 10 glucose, and 1.7 $CaCl_2$, gassed with 95% O_2/5% CO_2, filtered through a 5-μm filter to remove any particulate contaminants, pH 7.4] that was maintained at a constant temperature of 37°C and was gassed continuously for the entire duration of the experiment (29, 36). The aorta was cannulated, and retrograde perfusion in the Langendorff mode through the aortic cannula was initiated at a perfusion pressure of 100 mm Hg, followed by cannulation of pulmonary vein through the atrial cannula. After 10 min of retrograde perfusion, the heart was switched to antegrade perfusion mode, in which the KHB buffer entered the cannulated left atrium at a pressure equivalent to 17 cm of water and passed to the left ventricle, from which it was spontaneously ejected through the aortic cannula. At the end of 15 min (in working mode), after the attainment of steady-state cardiac function, baseline functional parameters were recorded. The circuit was then switched back to the retrograde mode. In the ischemia–reperfusion group (LZIR and BCTIR), the hearts were perfused for 60 min, followed by exposure to zero-flow normothermic global ischemia for 30 min, followed by 120 min of reperfusion. For the ischemic-preconditioning groups (LZIPIR and BCTIPIR), the hearts were subjected to four episodes of 5-min global ischemia followed by 10-min reperfusion before I/R. The first 10 min of reperfusion was in the retrograde mode to allow postischemic stabilization and thereafter in the antegrade working mode to allow assessment of functional parameters, which were recorded at 30-, 60-, 90-, and 120-min reperfusion (29, 36).

Cardiac functions

Aortic pressure was measured by using a pressure transducer (Micro-Med) connected to a sidearm of the aortic cannula, and the signal was amplified by using a Heart Performance Analyzer Model 400 (Micro-Med). Heart rate (HR), left ventricular developed pressure (LVDP), and dp/dt_{max} were all derived from the continuously obtained pressure signal. Aortic flow was measured by using a calibrated flow meter (Gilmont Instrument, Barrington, IL), and coronary flow was measured by timed collection of the coronary effluent dripping from the heart.

Estimation of infarct size

The infarct size was measured as previously described (29, 36). After reperfusion, hearts were immediately perfused with 1% triphenyltetrazolium chloride. The hearts were excised and stored at −70°C until sectioning. Later, each heart was sectioned into four to six sections of 1-mm thickness and fixed in 10% formalin, placed between two coverslips, and digitally imaged with the use of an Epson scanner. To quantitate the areas of interest in pixels, Scion Image (Beta 4.03 for Windows) analyzing software was used.

TUNEL assay for cardiomyocyte apoptosis

Formaldehyde-fixed heart tissue sections were embedded in paraffin, cut into transverse sections (4 μm thick), and deparaffinized with a graded series of histoclear and ethanol solutions. Immunohistochemical detection of apoptotic cells was carried out with a TUNEL reaction by using In Situ Cell Death Detection Kit, Fluorescein, as per the kit protocol (Roche Diagnostics, Mannheim, Germany). The sections ($n = 4$) were washed 3× in PBS, blocked with 10% normal goat serum in 1% BSA in PBS, and incubated with anti-α-sarcomeric actin (Sigma, St. Louis, MO) followed by staining with TRITC-conjugated rabbit anti-mouse IgG (1:200 dilution; Sigma). After incubation, the sections were rinsed thrice in PBS and mounted with Vectashield mounting medium (Vector, Burlingame, CA). Observed images were captured by using a confocal laser Zeiss LSM 410 microscope. For the quantitative purpose, the number of TUNEL-positive cardiomyocytes was counted in 100 high-power fields (HPFs) (36).

Immunohistochemistry for β-catenin expression

The paraffin-embedded sections from *ex vivo* hearts were used to study the expression of β-catenin (30). Myocardial sections were analyzed for the reactivity with 1:500 diluted monoclonal antibody against β-catenin (BD Transduction Labs, Lexington, KY). Bound antibody was detected with the Vectastain ABC kit (Vector Laboratories, Burlingame, CA) and visualized with DAB (Sigma).

Western blot analysis

To quantify the expression of VEGF, Bcl-2, Survivin, and β-catenin, we performed Western blot analysis by using various specific primary antibodies. In brief, left ventricular heart tissues from each treatment group were homogenized and suspended (50 mg/ml) in sample buffer [10 m*M* HEPES, pH 7.3, sucrose 11.5%, EDTA 1 m*M*, EGTA 1 m*M*, diisopropylfluorophosphate (DFP), pepstatin A 0.7 mg/ml, leupeptin 10 mg/ml, aprotinin 2 mg/ml]. The homogenates were subjected to subcellular fractionation followed by isolation of cytosolic and nuclear fractions, which were used for protein analysis. The total protein concentration was determined by using the BCA (bicin-

choninic acid) protein assay kit (Pierce, Rockville, IL). The cytosolic and nuclear proteins were run on polyacrylamide electrophoretic gels (SDS-PAGE) typically with 10% (acrylamide-to-bis ratios). The separated proteins were electrophoretically transferred to Immobilon-P membranes (Millipore Corp., Bedford, MA) by using a semidry transfer system (Bio-Rad, Hercules, CA). Protein standards (Bio-Rad) were run in each gel. The blots were blocked in Tris-buffered saline/Tween-20 (TBS-T containing 20 m*M* Tris base, pH 7.6, 137 m*M* NaCl, 0.1% Tween-20) supplemented with 5% (wt/vol) nonfat dry milk for 1 h; blots were incubated overnight at 4°C with VEGF (R&D Systems Inc., Minneapolis, MN), Bcl-2 (Santa Cruz Biotechnology), Survivin (Novus Biologicals, Littleton, CO), and β-catenin (Upstate, Lake Placid, NY) primary antibody. Membranes were washed 3 times in TBS-T before incubation for 1 h with horseradish peroxidase–conjugated secondary antibody diluted 1:2,000 in TBS-T and 5% (wt/vol) nonfat dry milk. After incubation, membranes were washed 3 times with TBS-T for 10 min each, blots were treated with Enhanced Chemi-Luminescence (Amersham, Piscataway, NJ) reagents, and the required proteins were detected by autoradiography for variable lengths of time with Kodak X-Omat film (21, 30, 36).

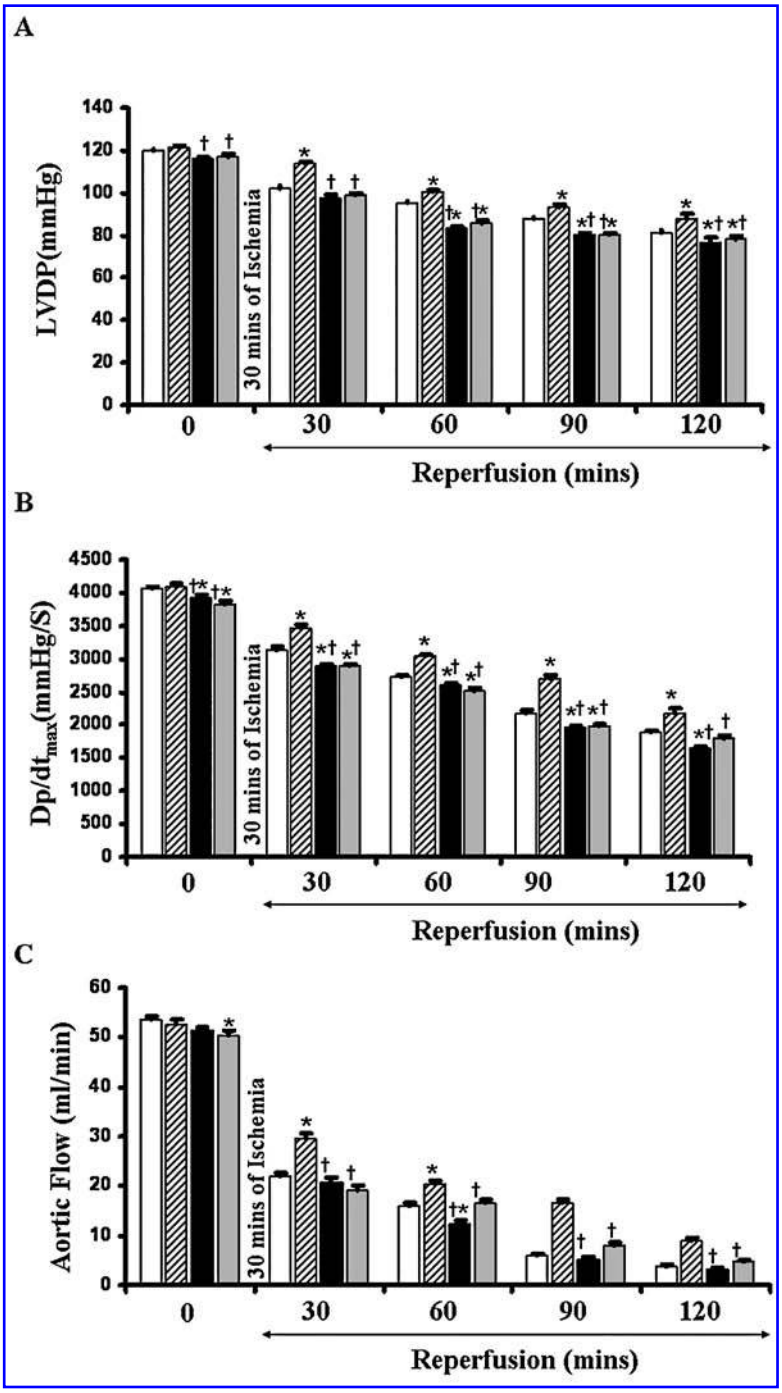

FIG. 1. Effect of Ad-sh-β-cat (BCT) on cardiac functional parameters at baseline (BL) and after 30 min of ischemia at 30, 60, 90, and 120 min of reperfusion. The results in (**A**) represent LVDP. (**B**) dp/dt_{max}. (**C**) Aortic flow. Results are shown in six animals per group. $^{*}p < 0.05$ represents comparison with LZIR. $^{\dagger}p < 0.05$ represents comparison with LZIPIR. *Blank bar*, LZIR; *wide upward diagonal bar*, LZIPIR; *black bar,* BCTIR; *grey bars*, BCTIPIR group.

Quantitative real-time RT-PCR for VEGF, Bcl-2, and Survivin

Reverse transcription reaction (RT) was performed with 1 μg total RNA isolated from left ventricular tissue of all the groups ($n = 6$ in each group). Real-time RT-PCR analysis was carried out with 10 ng of RT product by the iCycler iQ detection system (Biorad) by using Syber Green I fluorescence and β-actin as reference control. The primer sequences used for real-time RT-PCR for Rat VEGF F: TGTGCGGGCTGCTGCAATGAT, R: TGTGCTGGCTTTGGTGAGGTTTGA; Rat Bcl-2 F:CTTTGCAGAGATGTCC AGTCAG , R: GAACTCAAAGAAGGCCACAATC; and Rat Survivin F: CCTTTCTGGTCTTGATGTTTCC, R: ATTACCCCATGGTAGGAGGACT (21, 36).

Statistical analysis

The data are reported as mean ± standard error of the mean (± SEM). Measurements of the myocardial functional parameters at the different time points, infarct size, apoptosis, and QPCR analysis were analyzed with one-way analysis of variance (ANOVA) with Bonferroni corrections by using the statistical SPSS software. The results were considered significant if the p value was <0.05.

RESULTS

IP-mediated recovery of ventricular function is abolished by ad-sh-β-cat (BCT) after ischemia–reperfusion

No significant difference in baseline function was found among the four groups. Throughout the study, the heart rate and coronary flow were not significantly different between the two groups. The functional values of each parameter (such as LVDP, dp/dt_{max}, and aortic flow) were significantly decreased in all groups after 30 min of global ischemia, as expected, compared with their respective baseline values. Postischemic myocardial function was significantly deteriorated in the Ad-sh-βcat–injected groups, as evidenced by the significant decrease in left ventricular developed pressure (LVDP), dp/dt_{max}, and aortic flow (AF) compared with Adeno LacZ–injected groups. A significant decrease in LVDP (Fig. 1A) was observed throughout the reperfusion period. Values after 120 min of reperfusion for LVDP in BCTIR (76.67 ± 1.96 mm Hg) and BCTIPIR (78 ± 1.6 mm Hg) decreased compared with LZIR (81.16 ± 1.47 mm Hg) and LZIPIR (88.16 ± 2.04 mm Hg). A significant decrease in dp/dt_{max} (Fig. 1B) also was obtained throughout the reperfusion time after 120 min of reperfusion in both BCTIR (1,655 ± 77.2 mm Hg/sec) and BCTIPIR (1,802 ± 89.31 mm Hg/sec) as compared with the LZIR (1,881 ± 83.51 mm Hg/sec) and LZIPIR (2,189 ± 127.37 mm Hg/sec), respectively. Similarly, aortic flow (Fig. 1C) was significantly decreased after 120 min of reperfusion in both BCTIR (3.25 ± 0.5 ml/min) and BCTIPIR (4.8 ± 1.02 ml/min) compared with LZIR (3.93 ± 0.66 ml/min) and LZIPIR (9.08 ± 1.4 ml/min).

The extent of infarct size and cardiomyocyte apoptosis is increased by Ad-sh-β-cat (BCT) in IP

Infarct size expressed as percentage infarction relative to total area at risk was noticeably increased in groups BCTIR and BCTIPIR (44 and 42%) compared with respective controls LZIR and LZIPIR (39 and 24%) (Fig. 2). Apoptotic cardiomyocytes (Fig. 3A) were detected by using TUNEL staining in conjunction with staining for α-sarcomeric actin. The number of apoptotic cardiomyocytes was significantly increased in the BCTIR and BCTIPIR (111 and 122) groups when compared with the LZIR and LZIPIR (96 and 58) groups (Fig. 2B). Ad-sh-β-cat injection increased cardiomyocyte cell death due to apoptosis compared with Ad-LacZ–injected groups (Fig. 3B). It is also clear that IP-mediated cardioprotection is disrupted in the Ad-sh-β-cat–injected groups compared with controls.

β-Catenin nuclear translocation is inhibited by Ad-sh-β-cat (BCT) in IP

DAB staining for β-catenin showed *increased* translocation of β-catenin into the nucleus in Ad-LacZ–treated groups as compared with Ad-sh-β-cat–treated groups. LZIPIR showed *increased* translocation of β-catenin into the nucleus as compared with LZIR. After Ad-sh-β-cat injection, a reduction in β-catenin translocation was found as compared with corresponding Ad-LacZ controls, which demonstrates the inhibition of β-catenin protein expression as well as its translocation (Fig. 4).

mRNA expression of VEGF, Bcl-2, and survivin is inhibited by Ad-sh-β-cat (BCT) in IP

Real-time PCR results demonstrated a significant increase in the mRNA expression of VEGF (Fig. 5A) (1.61-fold), Bcl-2 (Fig. 5B) (1.6-fold), and survivin (Fig. 5C) (1.65-fold) in LZIPIR as compared with LZIR. BCTIR showed significant reduction in the mRNA expression of VEGF (0.57-fold), Bcl-2 (0.58-fold), and survivin (0.63-fold) as compared with LZIR.

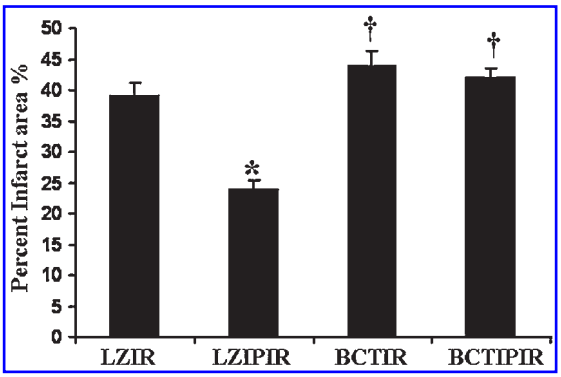

FIG. 2. Effect of Ad-sh-β-cat (BCT) on infarct size. Graph represents the percentage (%) of infarct size between the comparative groups after 30 min of ischemia and 2 h of reperfusion. Results are shown in six animals per group. $^{*}p < 0.05$ represents comparison with LZIR. $^{\dagger}p < 0.05$ represents comparison with LZIPIR.

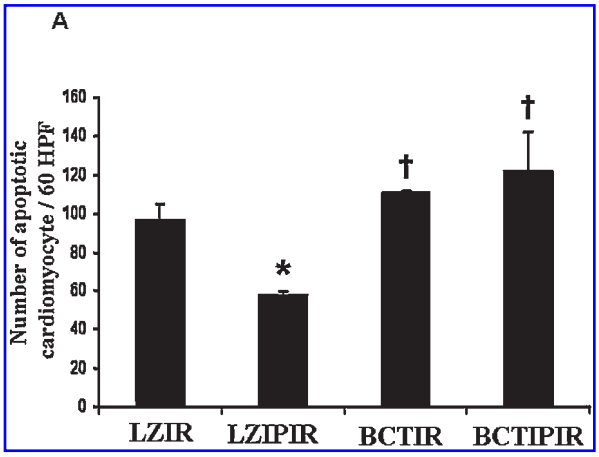

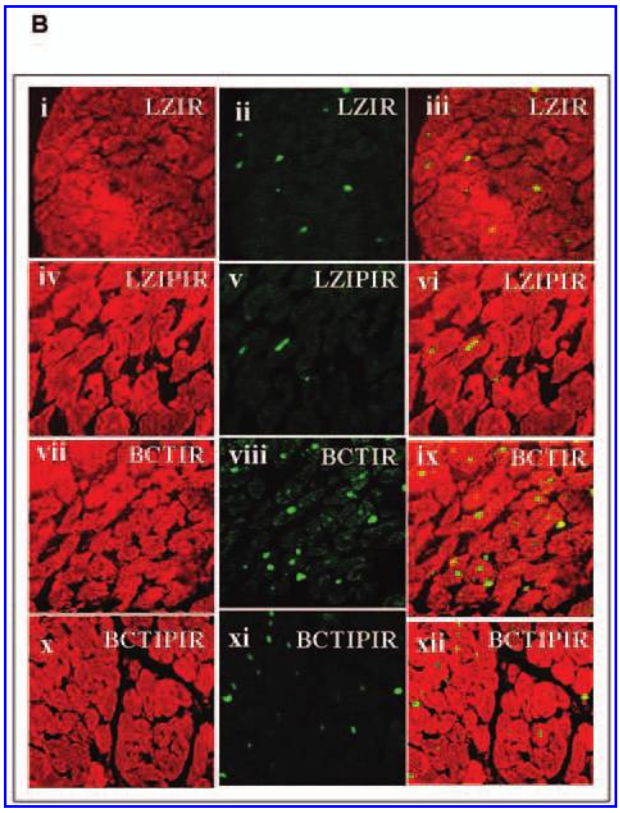

FIG. 3. (A) Effect of Ad-sh-β-cat (BCT) on cardiomyocyte apoptosis. Graph represents the number of cardiomyocyte apoptosis between the comparative groups after 30 min of ischemia and 2 h of reperfusion. Results are shown in six animals per group. $^{*}p < 0.05$ represents comparison with LZIR; $^{\dagger}p < 0.05$ represents comparison with LZIPIR. (**B**) Representative pictures of cardiomyocyte apoptosis. Apoptotic cells identified with anti-α sarcomeric actin labeling colocalizes with those identified with Tunel labeling. Rat heart sections were labeled with immunofluorescence and visualized by using confocal microscopy. Cross section of the fluorescently labeled vasculature demonstrates the presence of (I, IV, VII, and X, red fluorescence) and (II, V, VIII, and XI, green fluorescence). III, VI, IX, and XII show the superimposed pictures representing the apoptotic cardiomyocytes. (For interpretation of the references to color in this figure legend, the reader is referred to the web version of this article at www.liebertonline.com/ars).

Significant reduction in the mRNA expression of VEGF (0.9- *vs.* 1.61-fold), Bcl-2 (0.8- *vs.* 1.6-fold), and survivin (0.42- *vs.* 1.65-fold) was observed in BCTIPIR as compared with LZIPIR.

Inhibition of cytosolic and nuclear β-catenin protein expression by Ad-sh-β-cat (BCT) in IP

Western blot analysis of β-catenin in the nuclear fraction showed a significant increase in the β-catenin protein expression in LZIPIR (1.9-fold) as compared with LZIR (Fig. 5). Significant reduction in the β-catenin protein expression was observed in the BCTIR and BCTIPIR as compared with their corresponding control LacZ groups. Similar results were obtained even in the cytosolic fraction for β-catenin protein expression (Fig. 6).

Expression of VEGF, Bcl-2, and survivin inhibited by Ad-sh-β-cat (BCT) in IP

Western blot analysis for VEGF, Bcl-2, and survivin in the cytosolic fraction showed a significant increase in the expression these proteins to 2.1-, 1.2-, and 1.8-fold in LZIPIR as compared with LZIR. Significant reduction in the protein expression of VEGF (0.9- *vs.* 2.1-fold), Bcl-2 (0.9- *vs.* 1.2-fold), and survivin (1.3- *vs.* 1.8-fold) was observed in BCTIPIR as compared with LZIPIR (Fig. 7).

DISCUSSION

Our present findings highlight the importance of IP-mediated β-catenin signaling in cardioprotection. This study clearly shows that β-catenin plays an important role during ischemic

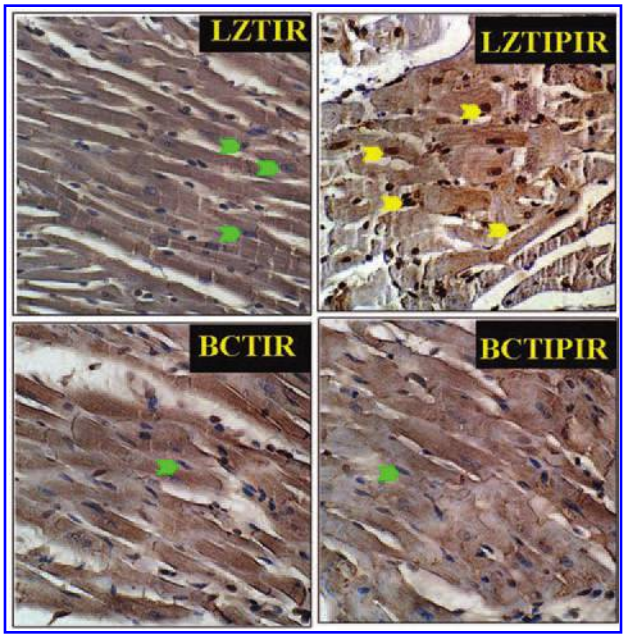

FIG. 4. Representative pictures of beta-catenin by using DAB staining. *Green arrows*, The β-catenin expression in the cytosol; *yellow arrows*, the β-catenin translocation into the nucleus. (For interpretation of the references to color in this figure legend, the reader is referred to the web version of this article at www.liebertonline.com/ars).

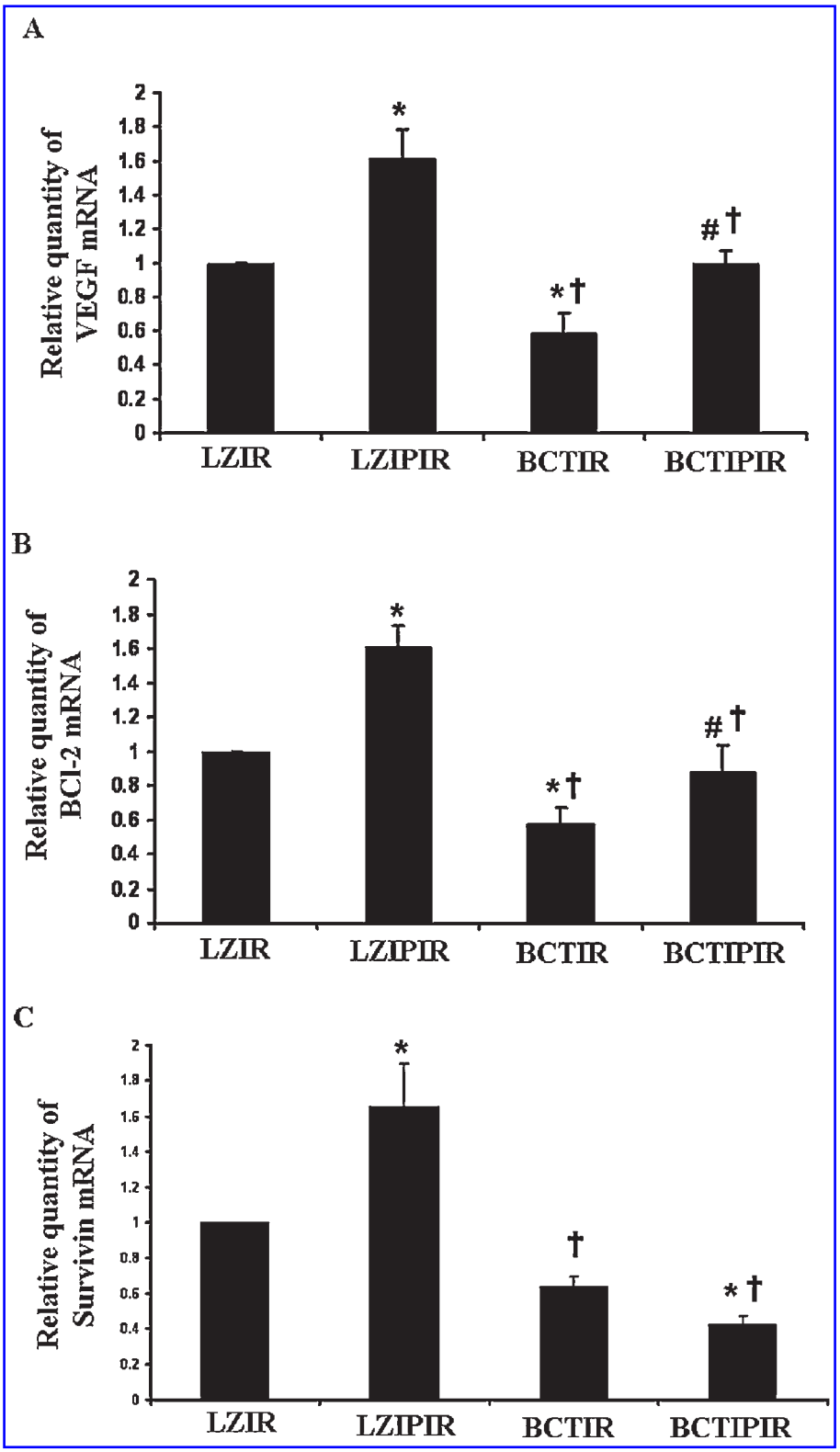

FIG. 5. Representative bar graphs showing the various mRNA expression. (**A**) VEGF. (**B**) Bcl-2. (**C**) Survivin. $^{*}p < 0.05$ represents comparison with LZIR. $^{\dagger}p < 0.05$ represents comparison with LZIPIR. $^{\#}p < 0.05$ represents comparison with BCTIR ($n = 6$).

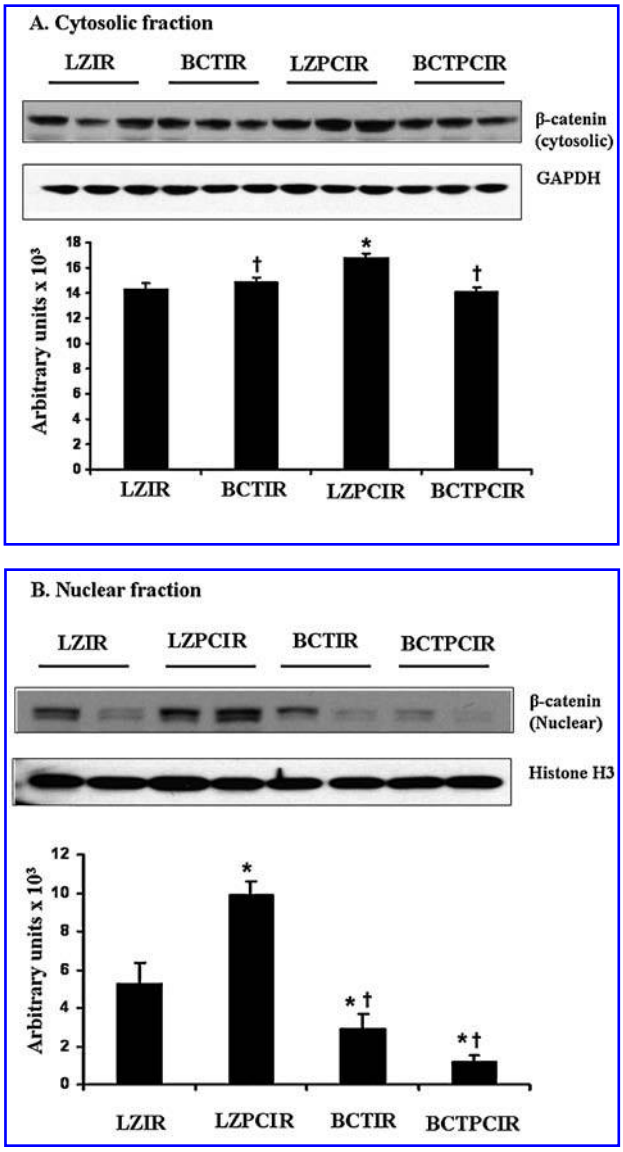

FIG. 6. (A) Representative Western blot showing the expression of β-catenin in the cytosolic fraction. GAPDH was used as the loading control. Bar graph represents the quantitative comparison between the groups. (**B**) Representative Western blot showing the expression of β-catenin in the nuclear fraction. Histone H3 was used as the loading control. Bar graph represents the quantitative comparison between the groups. $^{*}p < 0.05$ represents comparison with LZIR. $^{\dagger}p < 0.05$ represents comparison with LZIPIR. $^{\#}p < 0.05$ represents comparison with BCTIR ($n = 6$).

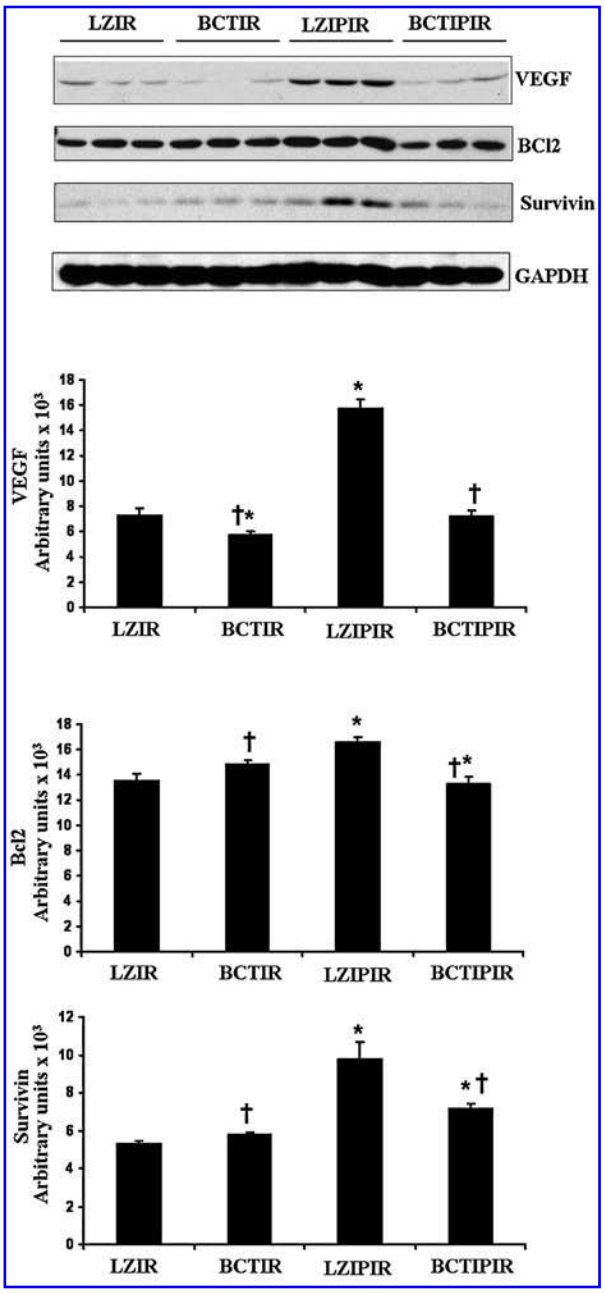

FIG. 7. Representative Western blot showing the expression of VEGF, Bcl-2, and survivin in the cytosolic fraction. GAPDH was used as the loading control. Bar graph represents the quantitative comparison between the groups for VEGF, Bcl-2, and survivin. $^{*}p < 0.05$ represents comparison with LZIR. $^{\dagger}p < 0.05$ represents comparison with LZIPIR. $^{\#}p < 0.05$ represents comparison with BCTIR ($n = 6$).

preconditioning by promoting survival signals through the induction of survivin, Bcl2, and VEGF expression. We demonstrated that silencing β-catenin 72 h before ischemia–reperfusion completely abolished the beneficial effect of IP, which is demonstrated by increased infarct size, apoptosis, and decreased myocardial functions.

In this study, we determined the mechanism by which β-catenin protects the myocardium from ischemic injury. The *in vitro* transfection efficiency of the shRNA was found to be ~85% (data not shown). There was a significant decrease in β-catenin (both at the mRNA and protein level) expression (not shown) 72 h after Ad-sh-β-catenin injection to the myocardium. On the basis of these results, we proceeded to *in vivo* studies using the same DNA sequences. In the present study, the physiological results revealed that the silencing of β-catenin in ischemic reperfused myocardium abolished IP-mediated cardiopro-

tection, as observed by a significant reduction in LVDP, dp/dt_{max}, and aortic flow compared to Ad-LacZIPIR. With regard to the cardiovascular effects of Ad-sh-β-catenin treatment, no evidence of any change in blood pressure or heart rate was noted.

Another interesting finding is that silencing of β-catenin in IP myocardium reduced proangiogenic and antiapoptotic molecules such as VEGF, Bcl2, and survivin, both at the mRNA and the protein levels. Exposure to IP probably stimulates an antiapoptotic and also angiogenic (PI3k/AKT and Wnt) pathway that promotes GSK-3β phosphorylation and thereby its inhibition. The inhibition of GSK3-β activity triggers β-catenin translocation to the nucleus and subsequently induces the activation of TCF-LEF transcription factors. Recently, GSK-3β was shown to play an important role in cardioprotection through its control of vascular cell migration and differentiation (23); however, the downstream targets that transmit proangiogenic or survival signaling have not been elucidated. Phosphorylation of GSK-3β at an amino-terminal Ser-9 residue by Akt results in the inhibition of GSK-3β (6).

β-Catenin is best known for its role in development and cancer. Generally, Wnts and β-catenin have been implicated in vascular development and remodeling (16, 20). β-Catenin can regulate vascular patterning through its role at the membrane sites of endothelial cell–cell attachment (5).

Ischemic stress probably induces the formation of a multiprotein complex that includes Axin, GSK-3β, and β-catenin. Surprisingly, the stabilization of the β-catenin–degradation complex (12), which is normally associated with destabilization of β-catenin, was associated with increased cytosolic levels (stabilization) of β-catenin by IP. In our previous report, the stabilization of β-catenin as observed in IP myocardium, achieved probably *via* Ser-9 phosphorylation of GSK-3β, and this, in turn, occurs *via* recruitment of Akt to the Axin. However, Wnts also stabilizes β-catenin *via* inhibition of GSK-3β, probably *via* different mechanism (10, 41). A number of studies demonstrated a key role for canonical Wnt signaling through β-catenin in stem cells from a variety of cell types (31). Inactivation of β-catenin–related genes results in the death of the embryo at gastrulation because of defects in anterior–posterior axis formation and mesoderm organization (14, 19). Besides its role as a cadherin partner, β-catenin is an important signaling and transcriptional factor. The absence of β-catenin (center piece) blocks Wnt signaling in endothelial cells, leading to a severely abnormal situation (25). Lampugnani *et al*. (13) demonstrated that in absence of β-catenin, VEGF receptor-2 signaling to cell proliferation is not inhibited by confluency. Therefore, uncontrolled endothelial cell proliferation may lead to irregular organization of the vasculature. Consistent with increased VEGF signaling, Skurke *et al*. (33) documented that β-catenin transduction induced upregulation of VEGFR2 transcript and protein levels in endothelial cells (33). Moreover, it was found that β-catenin increased VEGFR2 tyrosine phosphorylation and it is correlated with endothelial cell migration and tube formation. In another report, β-catenin was found to recruit PI3-kinase to VEGFR2, which led to the activation of a survival signal through AKT (28). It is our understanding through our findings and others that Wnt signaling and PI3-kinase/AKT signaling converge through β-catenin–mediated regulation of survival signal. Hence β-catenin plays a complex role in molecular signaling, which needs more attention.

In conclusion, our present study showed that silencing of β-catenin abolished IP-mediated cardioprotection, probably by the inhibition of survival molecules BCl2, survivin, and VEGF, both at the mRNA and protein levels, which initiated the death signal that was apparent from significantly increased infarct size and the extent of apoptosis. This is the first report of a positive role of β-catenin in cardioprotection, suggesting that β-catenin may act as a new therapeutic target for the cardiovascular system.

ACKNOWLEDGMENTS

This study was supported by National Institutes of Health grants HL 56803, HL 69910, and HL 85804.

ABBREVIATIONS

BCl2, B-cell CLL/lymphoma 2; BCT, β-catenin; BCTIPIR, adeno-sh-β-catenin–injected hearts subjected to ischemic preconditioning followed by ischemia–reperfusion; BCTIR, adeno-sh-β-catenin–injected hearts subjected to ischemia–reperfusion; BSA, bovine serum albumin; dp/dt_{max}, developed pressure/developed time; GSK3β, glycogen synthase kinase 3β; HR, heart rate; I, ischemia; IP, ischemic preconditioning; IPIR, ischemic preconditioning followed by ischemia–reperfusion; IR, ischemia–reperfusion; KHB, Krebs–Henseleit bicarbonate buffer; LVDP, left ventricular developed pressure; LZ, Lac-Z; LZIPIR, adeno Lac-Z–injected hearts subjected to ischemic preconditioning followed by ischemia–reperfusion; PBS, phosphate-buffered saline; PCR, polymerase chain reaction; R, reperfusion; VEGF, vascular endothelial growth factor.

REFERENCES

1. Aberle H, Bauer A, Stappert J, Kispert A, and Kemler R. beta-Catenin is a target for the ubiquitin-proteasome pathway. *EMBO J* 16: 3797–3804, 1997.
2. Alkhulaifi AM. Preconditioning the human heart during aorto-coronary bypass surgery. *J Cardiovasc Surg* 8: 270–275, 1994.
3. Behrens J, von Kries JP, Kühl M, Bruhn L, Wedlich D, Grosschedl R, and Birchmeier W. Functional interaction of bold beta-catenin with the transcription factor LEF-1. *Nature* 382: 638–642, 1996.
4. Bienz M. TCF: transcriptional activator or repressor? *Curr Opin Cell Biol* 10: 366–372, 1998.
5. Cattelino A, Liebner S, Gallini R, Zanetti A, Balconi G, Corsi A, Bianco P, Wolburg H, Moore R, Oreda B, Kemler R, and Dejana E. The conditional inactivation of the beta-catenin gene in endothelial cells causes a defective vascular pattern and increased vascular fragility. *J Cell Biol* 162: 1111–1122, 2003.
6. Dajani R, Fraser E, Roe SM, Young N, Good V, Dale TC, and Pearl LH. Crystal structure of glycogen synthase kinase 3 beta: structural basis for phosphate-primed substrate specificity and autoinhibition. *Cell* 105: 721–732, 2001.
7. Ding VW, Chen RH, and McCormick F. Differential regulation of glycogen synthase kinase 3β by insulin and WNT signaling. *J Biol Chem* 275: 32475–32481, 2000.
8. Easwaran V, Lee SH, Inge L, Guo L, Goldbeck C, Garrett E, Wiesmann M, Garcia PD, Fuller JH, and Chan V. β-Catenin regulates vascular endothelial growth factor expression in colon cancer. *Cancer Res* 63: 3145–3153, 2003.
9. Ferdinandy P, Schulz R, and Baxter GF. Interaction of cardiovascular risk factors with myocardial ischemia/reperfusion injury, preconditioning, and postconditioning. *Pharmacol Rev* 59: 418–458, 2007.

10. Frame S, Cohen P, and Biondi RM. A common phosphate binding site explains the unique substrate specificity of GSK3 and its inactivation by phosphorylation. *Mol Cell* 7: 1321–1327, 2001.
11. Fukuda S, Kaga S, Sasaki H, Zhan L, Zhu L, Otani H, Kalfin RK, Das D, and Maulik N. Angiogenic signal triggered by ischemic stress induces myocardial repair in rat during chronic infarction. *J Mol Cell Cardiol* 36: 547–559, 2004.
12. Gao ZH, Seeling JM, Hill V, Yochum A, and Virshup DM. Casein kinase I phosphorylates and destabilizes the beta-catenin degradation complex. *Proc Natl Acad Sci U S A* 99: 1182–1187, 2002.
13. Grazia Lampugnani M, Zanetti A, Corada M, Takahashi T, Balconi G, Breviario F, Orsenigo F, Cattelino A, Kemler R, Daniel TO, and Dejana E. Contact inhibition of VEGF-induced proliferation requires vascular endothelial cadherin, beta-catenin, and the phosphatase DEP-1/CD148. *J Cell Biol* 161: 793–804, 2003.
14. Haegel H, Larue L, Ohsugi M, Fedorov L, Herrenknecht K, and Kemler R. Lack of beta-catenin affects mouse development at gastrulation. *Development* 121: 3529–3537, 1995.
15. Halestrap AP, Clarke SJ, and Khaliulin I. The role of mitochondria in protection of the heart by preconditioning. *Biochim Biophys Acta* 1767: 1007–1031, 2007.
16. Hall RA and Lefkowitz RJ. Regulation of G protein-coupled receptor signaling by scaffold proteins. *Circ Res* 91: 672–680, 2002.
17. Hart MJ, de los Santos R, Albert IN, Rubinfeld B, and Polakis P. Downregulation of beta-catenin by human Axin and its association with the APC tumor suppressor, beta-catenin and GSK3 beta. *Curr Biol* 8: 573–581, 1998.
18. Hausenloy DJ, Tsang A, and Yellon DM. The reperfusion injury salvage kinase pathway: a common target for both ischemic preconditioning and postconditioning. *Trends Cardiovasc Med* 15: 69–75, 2005.
19. Huelsken J, Vogel R, Brinkmann V, Erdmann B, Birchmeier C, and Birchmeier W. Requirement for beta-catenin in anterior-posterior axis formation in mice. *J Cell Biol* 148: 567–578, 2000.
20. Ishikawa F, Miyazono K, Hellman U, Drexler H, Wernstedt C, Hagiwara K, Usuki K, Takaku F, Risau W, and Heldin CH. Identification of angiogenic activity and the cloning and expression of platelet-derived endothelial cell growth factor. *Nature* 338: 557–562, 1989.
21. Kaga S, Zhan L, Altaf E, and Maulik N. Glycogen synthase kinase-3β/β-catenin promotes angiogenic and anti-apoptotic signaling through the induction of VEGF, Bcl-2 and survivin expression in rat ischemic preconditioned myocardium. *J Mol Cell Cardiol* 40: 138–147, 2006.
22. Kawata H, Yoshida K, Kawamoto A, Kurioka H, Takase E, Sasaki Y, Hatanaka K, Kobayashi M, Ueyama T, and Hashimoto T. Ischemic preconditioning upregulates vascular endothelial growth factor mRNA expression and neovascularization via nuclear translocation of protein kinase Ce in the rat ischemic myocardium. *Circ Res* 88: 696–704, 2001.
23. Kim HS, Skurk C, Thomas SR, Bialik A, Suhara T, Kureishi Y, Birnbaum M, Keaney JF Jr, and Walsh K. Regulation of angiogenesis by glycogen synthase kinase-3beta. *J Biol Chem* 277: 41888–41896, 2002.
24. Kusano S and Raab-Traub N. I-mfa domain proteins interact with Axin and affect its regulation of the Wnt and c-Jun N-terminal kinase signaling pathways. *Mol Cell Biol* 22: 6393–6405, 2002.
25. Maretto S, Cordenonsi M, Dupont S, Braghetta P, Broccoli V, Hassan AB, Volpin D, Bressan GM, and Piccolo S. Mapping Wnt/beta-catenin signaling during mouse development and in colorectal tumors. *Proc Natl Acad Sci U S A* 100: 3299–3304, 2003.
26. Maulik N and Das DK. Potentiation of angiogenic response by ischemic and hypoxic preconditioning of the heart. *J Cell Mol Med* 6: 13–24, 2002.
27. Miller JR, Hocking AM, Brown JD, and Moon RT. Mechanism and function of signal transduction by the Wnt/beta-catenin and Wnt/Ca^{2+} pathways. *Oncogene* 18: 7860–7872, 1999.
28. Nawroth R, Poell G, Ranft A, Kloep S, Samulowitz U, Fachinger G, Golding M, Shima DT, Deutsch U, and Vestweber D. VE-PTP and VE-cadherin ectodomains interact to facilitate regulation of phosphorylation and cell contacts. *EMBO J* 21: 4885–4895, 2002.
29. Penumathsa SV, Koneru S, Thirunavukkarasu M, Zhan L, Prasad K, and Maulik N. Secoisolariciresinol diglucoside: relevance to angiogenesis and cardioprotection against ischemia-reperfusion injury. *J Pharmacol Exp Ther* 320: 951–959, 2007.
30. Penumathsa SV, Thirunavukkarasu M, Koneru S, Juhasz B, Zhan L, Pant R, Menon VP, Otani H, and Maulik N. Statin and resveratrol in combination induces cardioprotection against myocardial infarction in hypercholesterolemic rat. *J Mol Cell Cardiol* 42: 508–516, 2007.
31. Reya T and Clevers H. Wnt signalling in stem cells and cancer. *Nature* 434: 843–850, 2005.
32. Rubinfeld B, Albert I, Porfiri E, Fiol C, Munemitsu S, and Polakis P. Binding of GSK3beta to the APC-beta-catenin complex and regulation of complex assembly. *Science* 272: 974–975, 1996.
33. Skurk C, Maatz H, Rocnik E, Bialik A, Force T, and Walsh K. Glycogen-synthase kinase3beta/beta-catenin axis promotes angiogenesis through activation of vascular endothelial growth factor signaling in endothelial cells. *Circ Res* 96: 308–318, 2005.
34. Sui G, Shi Y. Gene silencing by a DNA vector-based RNAi technology. *Methods Mol Biol* 309: 205–218, 2005.
35. Sui G, Soohoo C, Affar el B, Gay F, Shi Y, Forrester WC, and Shi Y. A DNA vector based RNAi technology to suppress gene expression in mammalian cells. *Proc Natl Acad Sci U S A* 99: 5515–5520, 2002.
36. Thirunavukkarasu M, Penumathsa SV, Koneru S, Juhasz B, Zhan L, Otani H, Bagchi D, Das DK, and Maulik N. Resveratrol alleviates cardiac dysfunction in streptozotocin-induced diabetes: role of nitric oxide, thioredoxin, and heme oxygenase. *Free Radic Biol Med* 43: 720–729, 2007.
37. Tong H, Chen W, Steenbergen C, and Murphy E. Ischemic preconditioning activates phosphatidylinositol-3-kinase upstream of protein kinase C. *Circ Res* 87: 309–315, 2000.
38. Tong H, Imahashi K, Steenbergen C, and Murphy E. Phosphorylation of glycogen synthase kinase-3β during preconditioning through a phosphatidylinositol-3-kinase-dependent pathway is cardioprotective. *Circ Res* 90: 377-379, 2002.
39. Tsai JN, Lee CH, Jeng H, Chi WK, and Chang WC. Differential expression of glycogen synthase kinase 3 genes during zebrafish embryogenesis. *Mech Dev* 91: 387–391, 2000.
40. Yellon DM and Dana A. The preconditioning phenomenon: a tool for the scientist or a clinical reality? *Circ Res* 87: 543–550, 2000.
41. Yuan H, Mao J, Li L, and Wu D. Suppression of glycogen synthase kinase activity is not sufficient for leukemia enhancer factor-1 activation. *J Biol Chem* 274: 30419–30423, 1999.

Address reprint requests to:
Nilanjana Maulik, Ph.D., FACN, FICA
Department of Surgery
Molecular Cardiology and Angiogenesis Laboratory
University of Connecticut Health Center
263 Farmington Avenue
Farmington, CT 06030-1110

E-mail: nmaulik@neuron.uchc.edu

Date of first submission to ARS Central, February 7, 2008; date of final revised submission, March 18, 2008; date of acceptance, March 19, 2008.

This article has been cited by:

1. Qiao-ling Wu, Tu Shen, Li-li Shao, Hong Ma, Jun-ke Wang. 2012. Ischemic Postconditioning Mediates Cardioprotection Via PI3K/GSK-3#/#-Catenin Signaling Pathway in Ischemic Rat Myocardium. *Shock* **38**:2, 165-169. [CrossRef]
2. Mahesh Thirunavukkarasu, Ram Sudheer Adluri, Bela Juhasz, Samson Mathews Samuel, Lijun Zhan, Anupinder Kaur, Gautam Maulik, Juan A Sanchez, Janet Hager, Nilanjana Maulik. 2012. Novel role of NADPH oxidase in ischemic myocardium: a study with Nox2 knockout mice. *Functional & Integrative Genomics* **12**:3, 501-514. [CrossRef]
3. Yong-Xiang Xia, Ling Lu, Zheng-Shan Wu, Li-Yong Pu, Bei-Cheng Sun, Xue-Hao Wang. 2012. Inhibition of GSK-3# ameliorates hepatic ischemia-reperfusion injury through GSK-3#/#-catenin signaling pathway in mice. *Hepatobiliary & Pancreatic Diseases International* **11**:3, 278-284. [CrossRef]
4. Jae-Won Lee, Jong-In Kim, Young-Ah Lee, Dong-Hun Lee, Chang-Seon Song, Yoon Ju Cho, Jin Soo Han. 2012. Inhaled hydrogen gas therapy for prevention of testicular ischemia/reperfusion injury in rats. *Journal of Pediatric Surgery* **47**:4, 736. [CrossRef]
5. Piyajit Watcharasit, Sumitra Suntararuks, Daranee Visitnonthachai, Apinya Thiantanawat, Jutamaad Satayavivad. 2012. #-catenin involvement in arsenite-induced VEGF expression in neuroblastoma SH-SY5Y cells. *Environmental Toxicology* n/a-n/a. [CrossRef]
6. Ram Sudheer Adluri , Mahesh Thirunavukkarasu , Nageswara Rao Dunna , Lijun Zhan , Babatunde Oriowo , Kotaro Takeda , Juan A. Sanchez , Hajime Otani , Gautam Maulik , Guo-Hua Fong , Nilanjana Maulik . 2011. Disruption of Hypoxia-Inducible Transcription Factor-Prolyl Hydroxylase Domain-1 (PHD-1-/-) Attenuates Ex Vivo Myocardial Ischemia/Reperfusion Injury Through Hypoxia-Inducible Factor-1# Transcription Factor and Its Target Genes in Mice. *Antioxidants & Redox Signaling* **15**:7, 1789-1797. [Abstract] [Full Text HTML] [Full Text PDF] [Full Text PDF with Links]
7. Ram Sudheer Adluri, Mahesh Thirunavukkarasu, Lijun Zhan, Yuzo Akita, Samson Mathews Samuel, Hajime Otani, Ye-Shih Ho, Gautam Maulik, Nilanjana Maulik. 2011. Thioredoxin 1 enhances neovascularization and reduces ventricular remodeling during chronic myocardial infarction: A study using thioredoxin 1 transgenic mice. *Journal of Molecular and Cellular Cardiology* **50**:1, 239-247. [CrossRef]
8. Olivier Blanc-BrudeMyocardial Cell Death and Regeneration 66-80. [CrossRef]
9. Yu-Ping Wang, Peng-Zhou Hang, Li-Hua Sun, Yong Zhang, Jin-Long Zhao, Zhen-Wei Pan, Hong-Rui Ji, Li-An Wang, Hui Bi, Zhi-Min Du. 2009. M 3 muscarinic acetylcholine receptor is associated with #-catenin in ventricular myocytes during myocardial infarction in the rat. *Clinical and Experimental Pharmacology and Physiology* **36**:10, 995-1001. [CrossRef]